

## ARTICLE

## CO<sub>2</sub> Reduction with Protons and Electrons at a Boron-Based Reaction Center

Received 00th January 20xx,  
Accepted 00th January 20xx

DOI: 10.1039/x0xx00000x

Borohydrides are widely used reducing agents in chemical synthesis and have emerging energy applications as hydrogen storage materials and reagents for the reduction of CO<sub>2</sub>. Unfortunately, the high energy cost associated with the multistep preparation of borohydrides starting from alkali metals precludes large scale implementation of these latter uses. One potential solution to this issue is the direct synthesis of borohydrides from the protonation of reduced boron compounds. We herein report reactions of the redox series [Au(B<sub>2</sub>P<sub>2</sub>)<sup>n</sup>] ( $n = +1, 0, -1$ ) (B<sub>2</sub>P<sub>2</sub>, 9,10-bis(2-(diisopropylphosphino)phenyl)-9,10-dihydroboranthrene) and their conversion into corresponding mono- and diborohydride complexes. Crucially, the monoborohydride can be accessed via protonation of [Au(B<sub>2</sub>P<sub>2</sub>)<sup>-</sup>], a masked borane dianion equivalent accessible at relatively mild potentials (−2.05 V vs. Fc/Fc<sup>+</sup>). This species reduces CO<sub>2</sub> to produce the corresponding formate complex. Cleavage of the formate complex can be achieved by reduction (ca. −1.7 V vs. Fc/Fc<sup>+</sup>) or by the addition of electrophiles including H<sup>+</sup>. Additionally, direct reaction of [Au(B<sub>2</sub>P<sub>2</sub>)<sup>-</sup>] with CO<sub>2</sub> results in reductive disproportion to release CO and generate a carbonate complex. Together, these reactions constitute a synthetic cycle for CO<sub>2</sub> reduction at a boron-based reaction center that proceeds through a B–H unit generated via protonation of a reduced borane with weak organic acids.

### Introduction

Since their discovery by Schlesinger and Brown in the 1940s,<sup>1</sup> borohydrides have become ubiquitous reducing agents in the synthesis of fine and commodity chemicals.<sup>2</sup> More recently, borohydrides have attracted interest in energy storage applications,<sup>3</sup> both as a dense and readily handled source of H<sub>2</sub> and in the reduction of CO<sub>2</sub> to fuels such as formic acid and methanol.<sup>4</sup> The first report of the reaction of NaBH<sub>4</sub> with CO<sub>2</sub> dates back to 1955 when Wartick and Pearson described the solution (dimethyl ether) and solid-state reactions with mass-balance and hydrolytic analysis of the products.<sup>5</sup> In 1967, the reaction of NaBH<sub>4</sub> with CO<sub>2</sub> in aqueous conditions was shown to produce sodium formate.<sup>6</sup> The intrinsic role of the borohydride ion in CO<sub>2</sub> reduction was later investigated by Mizuta in 2014 who showed that, in the presence of a catalytic amount of NaBH<sub>4</sub>, BH<sub>3</sub> · THF effectively reduces CO<sub>2</sub> to trimethylboroxine.<sup>7</sup> A year later, Cummins reported the direct reaction of NaBH<sub>4</sub> with CO<sub>2</sub> yields the trisformatohydroborate that could be hydrolyzed to yield formic acid.<sup>8</sup> Additional studies over the last decade have found that in the presence of a suitable catalyst, pinacol borane (HBpin) and catechol borane (HBcat) can reduce CO<sub>2</sub> to a range of products<sup>9</sup> including carbon

monoxide<sup>10</sup> and formaldehyde,<sup>11</sup> formic acid,<sup>12</sup> and methanol equivalents.<sup>13</sup>

Despite their broad utility, one drawback to these reagents is the substantial energy required for their production. For example, millions of kg of NaBH<sub>4</sub> are produced each year by the NaH reduction of B(OMe)<sub>3</sub> in the Brown-Schlesinger process.<sup>14</sup>



NaH is prepared from the reaction of metallic Na with H<sub>2</sub> gas,<sup>14</sup> and the reduction of NaCl to metallic Na in the Downs Process. The process requires high temperature (>600 °C) and operating potentials of 8 V or more for practical reaction rates.<sup>15</sup> As a result, the stoichiometric reduction of CO<sub>2</sub> with NaBH<sub>4</sub>, or similarly produced B–H species,<sup>16</sup> entails a significant energy cost.

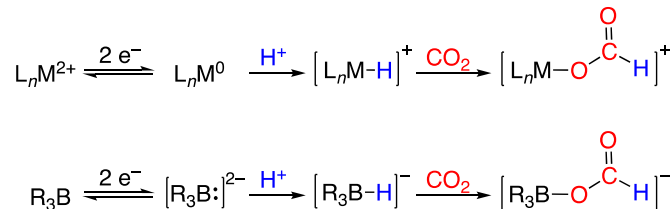


Figure 1. Redox-coupled hydride formation at a transition metal complex (top) and borane (bottom) as a strategy for CO<sub>2</sub> electroreduction to formate.

One potential solution to this issue would involve the direct construction of B–H bonds from the protonation of reduced boron compounds accessed at potentials tolerable to common solvents. Such a process would be analogous to the generation of transition metal hydrides via the reduction and protonation

<sup>a</sup> Department of Chemistry, University of California, Riverside, Riverside, California, 92521, United States. Email: hill.harman@ucr.edu

<sup>†</sup> Electronic Supplementary Information (ESI) available: Synthetic and experimental details and characterization data. X-ray crystallographic data is available from the CCDC under accession numbers 1921501–1921506. See DOI: 10.1039/x0xx00000x

of a transition metal complex (Figure 1). Despite the difficulty in accessing doubly reduced boranes,<sup>17</sup> there has been recent progress in the protonation of low valent boron compounds to generate B–H bonds (Figure 2). In 2006, Nozaki et al. reported the isolation of the boryllithium compound  $\text{LiB}(2,6\text{-iPrC}_6\text{H}_4)\text{NCH}_2)_2$ , which reacts as a boryl anion equivalent, and showed that it could be protonated with  $\text{H}_2\text{O}$  to give the corresponding hydroborane.<sup>18</sup> Bertrand et al. have prepared the carbene-stabilized borylene  $(\text{CAAC})_2\text{BH}$  ( $\text{CAAC}$  = cyclic (alkyl)(amino)carbene) that could be protonated with trifluoromethanesulfonic acid (TfOH) to yield the corresponding boronium salt.<sup>19</sup> A related bis(oxazol-2-ylidene)-phenylborylene system reported by Kinjo also produced a B–H moiety via protonation with TfOH.<sup>20</sup> Furthermore, Wagner synthesized a diborylmethane dianion and a doubly boron-doped dibenzo[*g,p*]chrysene dianion that could be protonated to yield the corresponding hydride bridged B–H–B species.<sup>21</sup> Additionally, Szymczak et al. reported a conceptually relevant series of Mn/Cr-borazine complexes that could be reduced and then protonated to yield a bridging metalloborohydride.<sup>22</sup> The reactivities (in particular, towards hydride transfer) of these B–H bonds formed via protonation have not been reported.

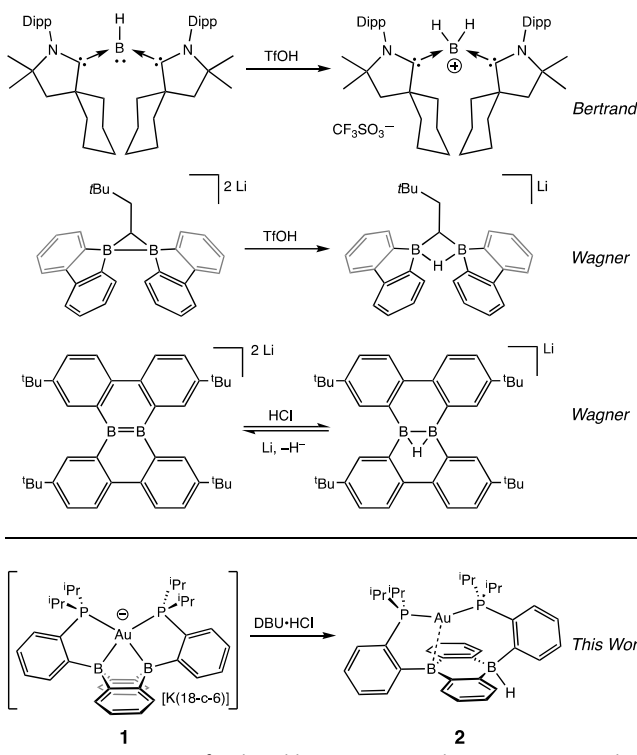


**Figure 2.** Protonation of reduced boron compounds to give tetracoordinate B–H moieties.

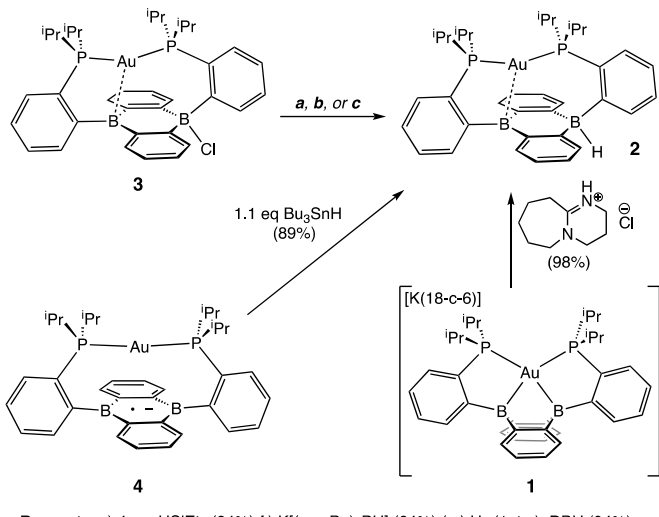
We recently reported the synthesis of the disphosphine tethered diboraanthracene ligand  $\text{B}_2\text{P}_2$  (9,10-bis(2-(diisopropylphosphino)phenyl)-9,10-dihydroboranthrene) and a series of its gold complexes in three states of charge. The anionic complex,  $[\text{Au}(\text{B}_2\text{P}_2)][\text{K}(18\text{-c-6})]$  (**1**), which features an unprecedented boroauride moiety, could be accessed at remarkably mild potentials (−2.05 V vs.  $\text{Fc}/\text{Fc}^+$ ,  $\text{MeCN}$ )<sup>23</sup> owing to the formation of a strong 3-centered, 2-electron bond between Au and the two B atoms.<sup>24</sup> Considering that **1** can be

thought of as a masked borane dianion, we wondered if protonation of this complex could provide direct access to a hydridic B–H unit (Figure 2). We herein report the synthesis and characterization of this borohydride complex,  $\text{Au}(\text{B}_2\text{P}_2)\text{H}$  (**2**), which can be generated via direct hydride reduction of  $\text{Au}(\text{B}_2\text{P}_2)\text{Cl}$  (**3**), FLP-type dihydrogen activation, H-atom addition to the boron-centered radical complex  $\text{Au}(\text{B}_2\text{P}_2)$  (**4**) or, most notably, by protonation of **1** with mild organic acids. Borohydride **2** is sufficiently reactive to reduce  $\text{CO}_2$  to formate, and cleavage of the resulting B–OCHO bond can be achieved either by addition of an electrophile (including  $\text{H}^+$ ) or by one electron reduction. These results collectively represent a synthetic cycle for  $\text{CO}_2$  reduction to formate with protons and electrons, with the key finding being the generation of a hydridic borohydride unit via protonation of a reduced borane at modest potentials. This reaction sequence, along with Wagner's recent reports of  $\text{CO}_2$  hydrogenation<sup>25</sup> and the reductive disproportionation of  $\text{CO}_2$ <sup>26</sup> catalyzed by DBA derivatives, illustrates the promise of redox-active boranes in the reduction of  $\text{CO}_2$ , an area dominated by transition metal chemistry.<sup>27</sup> Furthermore, given the recent application of boron-doped graphene to  $\text{CO}_2$  electroreduction,<sup>28</sup> these molecules offer well-defined molecular models<sup>29</sup> of fundamental chemical processes that may underlie small molecule reactivity at doped graphitic carbon surfaces.

## Results and discussion

Our initial synthetic approaches to a B–H containing derivative of  $\text{Au}(\text{B}_2\text{P}_2)$  began with direct hydride for halide substitution. Addition of 1 equiv.  $\text{K}[\text{sec-Bu}_3\text{BH}]$  to **3** gave borohydride **2** in 89% yield. This complex could also be prepared in good yield by exposing **3** to an excess of  $\text{Et}_3\text{SiH}$ . Additionally, **2** could be synthesized via frustrated Lewis pair (FLP)  $\text{H}_2$  activation in the presence of DBU (DBU = 1,8-diazabicyclo[5.4.0]undec-7-ene): exposure of a THF solution of equimolar **3** and DBU to 1 atm  $\text{H}_2$  resulted in the immediate formation of **2** as judged by  $^1\text{H}$ ,  $^{11}\text{B}$ , and  $^{31}\text{P}$  NMR spectroscopies. This reaction is presumably mediated by the pseudo-three-coordinate boron and is consistent with a relatively weak Au–B interaction in **3**. Single-crystal X-ray diffraction (XRD) studies of **2** show it to be a zwitterion in the solid state with an intact B–H bond on the DBA face opposite the Au center, analogous to the previously reported structure of zwitterion **3** (Figure 3). The H atom was located in the electron difference map and is bound to a quasi-tetrahedral B atom ( $\Sigma\angle\text{C-B-C} = 340.5^\circ$ ). On the opposite side of the DBA linker, the Au ion is bound by both P donors in a roughly linear fashion ( $\angle\text{P-Au-P} = 156.8^\circ$ ) with a single Au–B interaction ( $d_{\text{AuB}} = 2.644(1)$  Å) to one nearly-planar B atom ( $\Sigma\angle\text{C-B-C} = 359.8^\circ$ ). The  $^1\text{H}$  NMR spectrum of **2** features a signal at 5.09 ppm for a B–H proton resonance with the expected four-line pattern for coupling to a single  $^{11}\text{B}$  atom ( $J_{\text{BH}} = 80$  Hz). The  $^{11}\text{B}$  NMR shows a corresponding doublet at −10.01 ppm ( $J_{\text{BH}} = 80$  Hz) while the  $^{31}\text{P}$  NMR spectrum features two doublets at 58.4 and 55.9 ppm ( $J_{\text{PP}} = 255.0$  Hz), consistent with inequivalent phosphine ligands on the NMR timescale. Given the precedent for H-atom transfer reactivity at boron,<sup>30</sup> we also

targeted the synthesis of **2** from the neutral radical species **4** via H-atom addition. Reaction of  $\text{Au}(\text{B}_2\text{P}_2)$  with one equivalent of  $\text{Bu}_3\text{SnH}$  produces **2** and  $\text{Bu}_6\text{Sn}_2$  over 12 hours via apparent H-atom transfer as judged by NMR of reaction mixtures.



**Scheme 1.** Synthesis of  $\text{Au}(\text{B}_2\text{P}_2)\text{H}$  from  $\text{H}^-$ ,  $\text{H}^*$ , and  $\text{H}^+$

To probe the synthesis of **2** via protonation of **1**, we exposed **1** to a series of organic acids. Addition of one equivalent of solid  $[\text{Ph}_2\text{NH}_2]\text{Cl}$  or  $[\text{2,6-Me}_2\text{pyH}]\text{Cl}$  to  $\text{CD}_3\text{CN}$  solutions of **1** resulted in immediate effervescence and formation of dark purple reaction mixtures which were revealed by NMR analysis to contain a mixture of  $\text{H}_2$ , **3**, and **4**. Fortunately, addition of one equivalent of  $\text{DBU}\bullet\text{HCl}$  to a solution **1** in  $\text{CD}_3\text{CN}$  gave rise to a pale-yellow solution exhibiting  $^1\text{H}$ ,  $^{11}\text{B}$ , and  $^{31}\text{P}$  NMR resonances that matched authentic samples of **2** (Figures S5–7.) with no  $\text{H}_2$  observed. Furthermore, **2** is stable to treatment with excess  $\text{DBU}\bullet\text{HCl}$ .

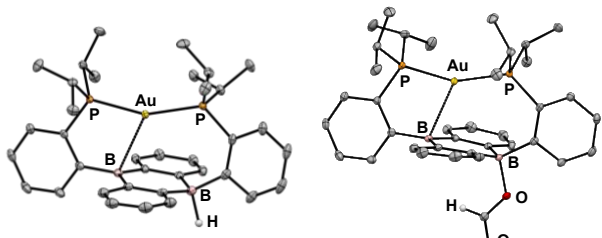
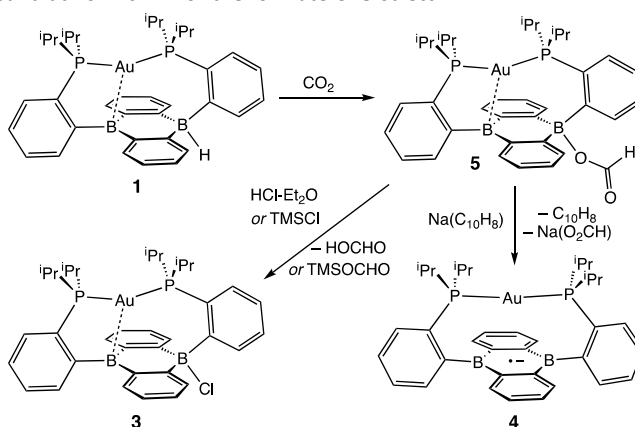


**Figure 3.** Thermal ellipsoid plots (50%) of  $\text{Au}(\text{B}_2\text{P}_2)\text{H}$  (**2**, left) and  $\text{Au}(\text{B}_2\text{P}_2)(\text{O}_2\text{CH})$  (**5**, right). Unlabeled ellipsoids correspond to carbon. Solvent molecules and most hydrogen atoms have been omitted for clarity.

With borohydride **2** in hand, we examined its reactivity with  $\text{CO}_2$ . Exposure of a  $\text{C}_6\text{D}_6$  solution of **2** to 1 atm of  $\text{CO}_2$  resulted in quantitative formation of the corresponding formate complex  $\text{Au}(\text{B}_2\text{P}_2)(\text{O}_2\text{CH})$  (**5**) within seconds. The solid-state structure of **5** confirms the insertion of  $\text{CO}_2$  into the B–H bond, with the resulting formate ion bound through a single O to one boron atom (Figure 3). The zwitterionic structure of **5** is analogous to **2** and **3**, with a tetrahedral boron center bound to the formate oxygen ( $\Sigma\angle\text{C-B-C} = 339.1^\circ$ ) and an intermediate length contact between Au and the non-formate bound B atom ( $d_{\text{AuB}} = 2.632 \text{ \AA}$ ). The  $^1\text{H}$  NMR spectrum of **5** in  $\text{CDCl}_3$  is consistent with  $C_{2v}$  symmetry in solution, with a lone singlet in the  $^{31}\text{P}$  NMR spectrum at 56.1 ppm and  $^{11}\text{B}\{^1\text{H}\}$  NMR displaying a

broad singlet at 26.9 ppm. Similar to **3**, the observed  $C_{2v}$  symmetry in solution along with a  $^{11}\text{B}$  chemical shift between that of bona fide three- and four-coordinate B centers in DBA containing molecules<sup>17h,f</sup> implies rapid exchange of the formate ion between each boron site of the DBA ring, a phenomenon also observed in **3**.<sup>22</sup> The  $^{13}\text{C}\{^1\text{H}\}$  NMR spectrum of **5** contains a resonance at 168.2 ppm corresponding to the formate carbon atom, and FTIR spectroscopy revealed a strong band at  $1672 \text{ cm}^{-1}$  for the formate C=O stretch.



**Scheme 2.**  $\text{CO}_2$  Reduction to Formate by  $\text{Au}(\text{B}_2\text{P}_2)\text{H}$

Next, we assessed the ability of electrophiles such as TMSCl and HCl to effect B–O bond scission. Treatment of **5** with excess TMSCl resulted in the immediate formation of **3** as judged by  $^1\text{H}$  and  $^{31}\text{P}$  NMR along with new resonances for trimethylsilylformate (Figure S13), accomplishing the net hydrosilylation of  $\text{CO}_2$ .<sup>31</sup> While silyl electrophiles have strong precedent to mediate E–O bond cleavage in main group systems,<sup>32</sup> we wondered if a suitable acid would be able to protonate the B–OCHO bond to yield formic acid. To this end, addition of  $[\text{Ph}_2\text{NH}_2]\text{Cl}$  or  $\text{DBU}\bullet\text{HCl}$  to  $\text{CDCl}_3$  solutions of **5** saw no observable reaction over the course of days at room temperature. However, addition of one equivalent of  $\text{HCl}\bullet\text{Et}_2\text{O}$  to **5** resulted in the immediate formation of the chloride complex **3** by  $^1\text{H}$  and  $^{31}\text{P}$  NMR spectroscopy with resonances for  $\text{HCO}_2\text{H}$  observed in the  $^1\text{H}$  NMR spectrum.

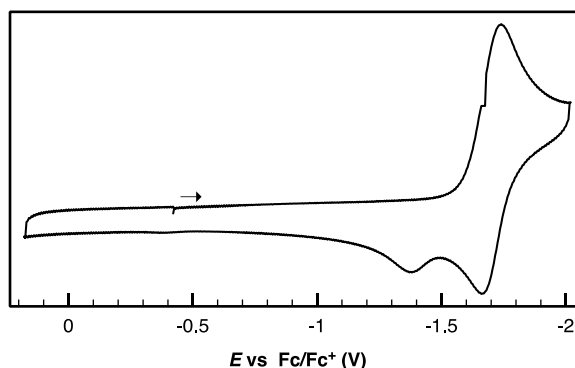


**Figure 4.** Cyclic voltammogram of  $\text{Au}(\text{B}_2\text{P}_2)(\text{O}_2\text{CH})$  performed in  $0.1 \text{ M } [\text{Bu}_4\text{N}]\text{[PF}_6]$  in  $\text{CH}_3\text{CN}$  at a scan rate of  $100 \text{ mV/s}$ .

Following successful electrophilic B–O bond cleavage in **5** to yield **3**, the reductive cleavage of the B–OCHO unit was explored. Cyclic voltammetry (CV) performed on **5** revealed a quasireversible process

at  $E_{1/2} = -1.74$  V vs.  $\text{Fc}/\text{Fc}^+$  which gave rise to an oxidative daughter wave at ca. -1.5 V (Figure 4). This daughter wave occurs at roughly the same potential as the oxidation of  $[\text{Au}(\text{B}_2\text{P}_2)]^{0+1}$ , consistent with the hypothesis that one electron reduction of **5** forms **[5]<sup>-</sup>** which then undergoes formate dissociation on the CV timescale to afford neutral **4**. To unambiguously confirm the liberation of formate ion, **5** was treated with 1 equivalent of  $\text{Na}(\text{C}_{10}\text{H}_8)$  in THF. A turbid, dark-purple solution immediately formed, indicating formation of **4**. The precipitated solids were collected by filtration and dissolved in  $\text{D}_2\text{O}$  with  $^1\text{H}$  NMR analysis revealing formation of  $\text{NaCO}_2\text{H}$  (Figure S12). To our knowledge, this is the only example of reductive cleavage of a B–OCHO bond to yield formate. This process is presumably driven by the accessible one-electron reduction chemistry of **5** (-1.74 V vs.  $\text{Fc}/\text{Fc}^+$ ) enabled by the DBA core and speaks to the utility of frontier orbital modulation by incorporation of boron into polycyclic aromatic hydrocarbon frameworks.<sup>33</sup> Collectively, these results outline a synthetic cycle for  $\text{CO}_2$  reduction with protons and electrons mediated exclusively at boron (Figure 5).

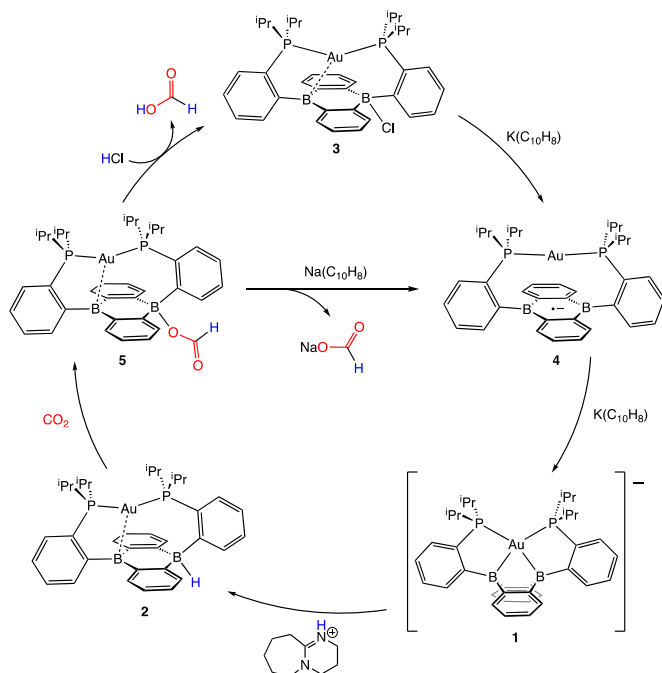
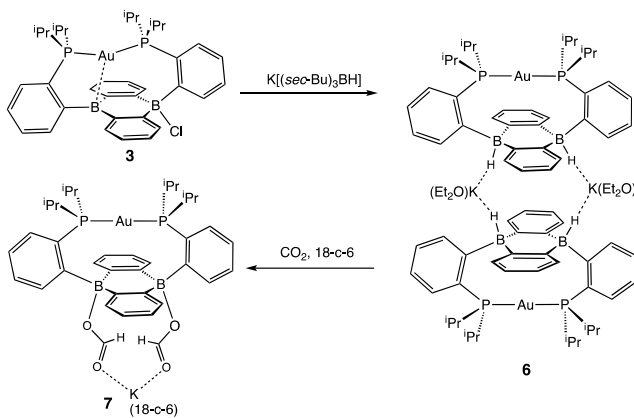


**Figure 5.** A closed synthetic cycle for the reduction of  $\text{CO}_2$  to formic acid with protons and electrons mediated by a redox active, metal-stabilized diboraanthracene platform.

In addition to the monoborohydride chemistry described above, we were able to generate a diborohydride species via formal sequential hydride addition to **3**. Two equivalents of  $\text{K}[\text{sec-Bu}_3\text{BH}]$  reacted with **3** in  $\text{Et}_2\text{O}$  to give the anionic diborohydride complex  $[\text{Au}(\text{B}_2\text{P}_2)\text{H}_2][\text{K}(\text{Et}_2\text{O})]$  (**6**). Single-crystal XRD reveals **6** to be a dimer in the solid state, (Figure 6) with two  $[\text{Au}(\text{B}_2\text{P}_2)\text{H}_2]^-$  units bridged by two  $[\text{K}(\text{Et}_2\text{O})]^+$  cations via contacts between the B–H and K atoms. The  $[(\text{Au}(\text{B}_2\text{P}_2)\text{H}_2)^-]$  component features a linear P–Au–P moiety ( $\angle \text{P–Au–P} = 161.9^\circ$ ) that sits above the DBA core with no appreciable interaction between Au and B ( $d_{\text{AuB}} > 3.25$  Å). The H atoms bound to both B centers exhibit a pseudo-tetrahedral geometry ( $\sum \angle \text{C–B–C} = 337.5^\circ$ ).  $^1\text{H}$  and  $^{11}\text{B}$  NMR spectra feature a 4-line pattern and

doublet, respectively, for the B–H moieties in **6**, analogous to the monoborohydride **2** (Figure S14). Compound **6** is structurally related to the diborohydride species resulting from  $\text{H}_2$  activation by reduced DBA compounds reported by Wagner.<sup>34</sup>

Diborohydride **6** is also reactive towards  $\text{CO}_2$  (1 atm), cleanly generating the corresponding diformate complex, which was isolated as its 18-crown-6 adduct,  $[\text{Au}(\text{B}_2\text{P}_2)(\text{O}_2\text{CH}_2)][\text{K}(18\text{-c-6})]$  (**7**). Single-crystal XRD confirmed the insertion of  $\text{CO}_2$  into both B–H bonds, with B atoms puckered out of planarity to accommodate each OCHO unit. Additionally, the formate moieties in **7** were identified by  $^1\text{H}$  NMR (8.34 ppm),  $^{13}\text{C}[^1\text{H}]$  NMR (168.2 ppm) and FTIR spectroscopy ( $\text{C=O}$ , 1672  $\text{cm}^{-1}$ ).



**Scheme 3.** Synthesis of Diborohydride **6** and its Reactivity with  $\text{CO}_2$

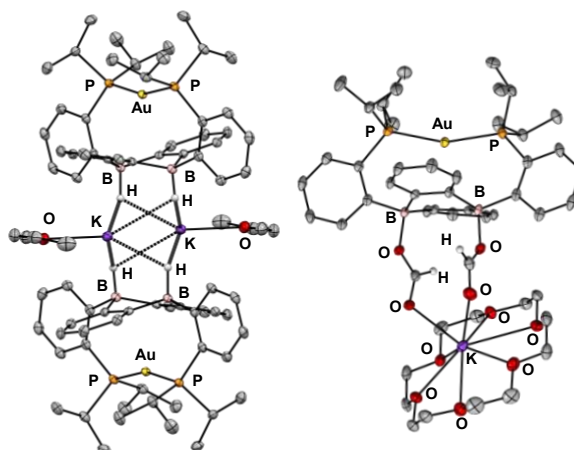
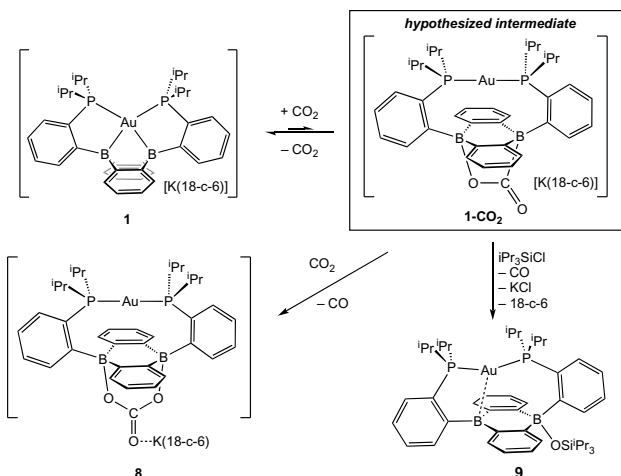


**Figure 6.** Thermal ellipsoid plots (50%) of the dimer of  $[\text{Au}(\text{B}_2\text{P}_2)\text{H}_2][\text{K}(\text{Et}_2\text{O})]$  (**6**, left) and  $[\text{Au}(\text{B}_2\text{P}_2)(\text{O}_2\text{CH}_2)][\text{K}(18\text{-c-6})]$  (**7**, right). Unlabeled ellipsoids correspond to carbon. Solvent molecules, a disordered crown ether component in **6**, and most hydrogen atoms have been omitted for clarity.

Having probed the  $[\text{Au}(\text{B}_2\text{P}_2)]$  system for  $\text{CO}_2$  reduction chemistry from its mono- and dihydrides, we additionally explored the direct reaction of  $\text{CO}_2$  with **1**. Wagner et al. recently reported that 9,10-dilithio-9,10-diborataanthracene reacts with  $\text{CO}_2$  to yield  $\text{CO}_3$  and  $\text{CO}$  via reductive disproportionation.<sup>25a</sup> Reaction of **1** with 1 atm of  $\text{CO}_2$  in  $\text{C}_6\text{D}_6$  resulted in the immediate formation of a colorless solution with no detectable precipitate. A single crystal suitable for XRD studies was obtained from  $\text{CO}_2$  saturated reaction mixtures and revealed the product to be the carbonate adduct,  $[\text{Au}(\text{B}_2\text{P}_2)\text{CO}_3][\text{K}(18\text{-c-6})]$  (**8**, Figure 7). The asymmetric unit of **8**

contains two crystallographically distinct molecules which are chemically equivalent in gross terms but exhibit minor differences in their geometries, most notably in their B–O distances, which range from 1.550(6) Å to 1.578(8) Å. This spread of B–O distances is consistent with a soft  $[\text{CO}_3]^{2-}$  binding potential, in agreement with Wagner's results.<sup>25a</sup> Solution NMR spectroscopy of **8** is consistent with  $C_{2v}$  symmetry and the  $[\text{CO}_3]^{2-}$  unit was identified by  $^{13}\text{C}\{^1\text{H}\}$  NMR (168.0 ppm) and FTIR (1592 cm<sup>-1</sup>) spectroscopies with  $^{13}\text{CO}_2$  experiments confirming these assignments (see SI).



**Scheme 4.** Reduction of  $\text{CO}_2$  to  $\text{CO}$  by  $[\text{Au}(\text{B}_2\text{P}_2)]^-$

In order to probe the mechanism of the formation of **8** from **1** and  $\text{CO}_2$ , we explored the reaction by NMR spectroscopy at low temperature. Recent reports on reduced boron-containing heterocycles,<sup>21</sup> offer extensive precedent for the cycloaddition of  $\text{CO}_2$  across the boron atoms, and we sought to probe whether a similar  $\text{CO}_2$  adduct,  $[\text{Au}(\text{B}_2\text{P}_2)\text{CO}_2]^-$  (**1-CO<sub>2</sub>**), might be an intermediate in the formation of **8**. Addition of a single equivalent of  $\text{CO}_2$  to a frozen solution of the anion **1** in  $d_8$ -toluene followed by insertion into a precooled ( $-50$  °C) NMR spectrometer and subsequent variable temperature NMR monitoring resulted in a 1:1 mixture of starting material **1** and the carbonate adduct **8**. When the same experiment was carried out with  $^{13}\text{CO}_2$  enhanced intensity was observed corresponding to the  $\text{Au}(\text{B}_2\text{P}_2)^{13}\text{CO}_3$  resonance at 168.2 ppm along with free  $^{13}\text{CO}$  at 184.5 ppm. These results are consistent with endergonic binding of  $\text{CO}_2$  to the DBA core followed by rapid reaction with a second equivalent of  $\text{CO}_2$  to release  $\text{CO}$  and form **8** (Scheme 4), analogous to the mechanism established by Wagner in a related system.<sup>25a</sup> As we were unable to observe the putative  $\text{CO}_2$  adduct  $[\text{Au}(\text{B}_2\text{P}_2)\text{CO}_2]^-$ , we attempted to trap it by other chemical means during the reaction of **1** with  $\text{CO}_2$ . Solutions of **1** are stable in the presence of triisopropylsilylchloride (TIPSCl); however, addition of 1 atm  $\text{CO}_2$  to a thawing  $\text{C}_6\text{D}_6$  solution of **1** and TIPSCl resulted in the immediate formation of a pale-yellow solution. Single-crystal XRD studies revealed the product to be the zwitterion  $\text{Au}(\text{B}_2\text{P}_2)(\text{OSiPr}_3)$  (**9**), which contains a triisopropylsiloxyde anion bound to one B atom (Figure 7). The  $^{31}\text{P}$  NMR spectrum contains a set of doublets at 56.0 ( $J_{\text{P-P}} = 240$  Hz) and 52.5 ( $J_{\text{P-P}} = 240$  Hz) ppm while the  $^{11}\text{B}$  NMR spectrum featured a broad resonance

at 51.5 and a sharper singlet at 2.99 ppm. Two crystallographically distinct molecules of **9** are present in the asymmetric unit although their geometries are essentially identical (Figure S44). The formation of **9** occurs with  $\text{CO}_2$  loss as judged by  $^{13}\text{CO}_2$  labeling experiments. Exposure of **9** to additional  $\text{CO}_2$  (1 atm) did not lead to any further reaction, ruling out additional reaction of the -OTIPS moiety with  $\text{CO}_2$  as has been previously observed for metal-siloxide units.<sup>35</sup>

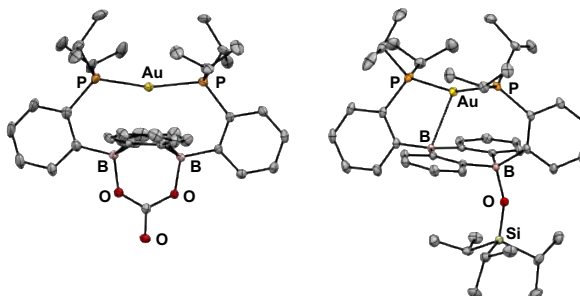


**Figure 7.** Thermal ellipsoid plots (50%) of the anion  $[\text{Au}(\text{B}_2\text{P}_2)(\text{CO}_3)][\text{K}(18\text{-c-6})]$  (**8**, left) and  $\text{Au}(\text{B}_2\text{P}_2)(\text{OSiPr}_3)$  (**9**, right). Unlabeled ellipsoids correspond to carbon. Solvent molecules, disordered components, and hydrogen atoms have been omitted for clarity.

## Conclusions

In conclusion, we have synthesized a reactive borohydride complex, **2**, via formal hydride addition, dihydrogen activation, radical H-atom addition, and, most crucially, reduction/protonation. The borohydride unit rapidly inserts  $\text{CO}_2$  to afford the formate complex **5**. Both CV and synthetic studies confirm that **5** can be reduced at  $E_{1/2} = -1.79$  V vs.  $\text{Fc}/\text{Fc}^+$  and undergo formate loss to give the neutral radical **4** and formate via reductive B–O cleavage. The cleavage of the B–O bond in **5** can also be achieved via addition of electrophiles including TMSCl or  $\text{HCl} \bullet \text{Et}_2\text{O}$ , to give **3** and TMSOCHO or formic acid, respectively. Additionally, direct reaction of the anion **1** with 1 atm of  $\text{CO}_2$  results in the extrusion of  $\text{CO}$  and the formation of carbonate complex **8** via the reductive disproportionation of  $\text{CO}_2$ . Collectively, these reactions outline a strategy for the reduction of  $\text{CO}_2$  with protons and electrons via reactive borohydride species generated at redox-active, conjugated boranes, and efforts to extend this chemistry to electrocatalytic systems are underway.

## Conflicts of interest

There are no conflicts to declare.

## Acknowledgements

This research was supported by the National Science Foundation (CHE-1752876) and the American Chemical Society Petroleum Research Fund (57314). NMR spectra were collected on instruments funded by an NSF MRI award (CHE-162673) and an Army Research Office instrumentation grant (W911NF-16-1-0523). W.H.H. is a member of the University of California, Riverside Center for Catalysis. Dr. Fook Tham and Dr. Charlene Tsay are acknowledged for X-ray crystallographic analysis

## Notes and references

<sup>1</sup> H. I. Schlesinger, H. C. Brown *J. Am. Chem. Soc.* 1940, **62**, 3429.

<sup>2</sup> (a) H. C. Brown, S. Krishnamurthy, *Tetrahedron* 1979, **35**, 567. (b) H. C. Brown, E. J. Mead, B. C. Subba Rao, *J. Am. Chem. Soc.* 1955, **77**, 6209.

<sup>3</sup> (a) J. Ma, N. A. Choudhury, Y. Sahai, *Renew. Sust. Energ. Rev.* 2010, **14**, 183. (b) M. Paskevicius, L. H. Jepsen, P. Schouwink, R. Cerny, D. Ravnsbaek, Y. Filinchuk, M. Dornheim, F. Besenbacher, T. R. Jensen, *Chem. Soc. Rev.* 2017, **46**, 1565.

<sup>4</sup> S. Bontemps, *Coord. Chem. Rev.* 2016, **308**, 117.

<sup>5</sup> (a) T. Wartik, R. K. Pearson, *J. Am. Chem. Soc.* 1955, **77**, 1075. (b) T. Wartik, R. K. Pearson, *J. Inorg. Nucl. Chem.* 1958, **7**, 404.

<sup>6</sup> F. Eisenberg Jr., A. H. Bolden, *Carbohydr. Res.* 1967, **5**, 349–350.

<sup>7</sup> K. Fujiwara, S. Yasuda, T. Mizuta, *Organometallics* 2014, **33**, 6692.

<sup>8</sup> I. Knopf, C. Cummins, *Organometallics* 2015, **34**, 1601.

<sup>9</sup> S. Bontemps, *Coord. Chem. Rev.* 2016, **308**, 117–130.

<sup>10</sup> (a) D. S. Laitar, P. Muller, J. P. Sadighi, *J. Am. Chem. Soc.* 2005, **127**, 17196. (b) H. Zhao, Z. Lin, T. B. Marder, *J. Am. Chem. Soc.* 2006, **128**, 15637.

<sup>11</sup> S. Bontemps, L. Vendler, S. Sabo-Etienne, *Angew. Chem. Int. Ed.* 2012, **124**, 1703.

<sup>12</sup> (a) M.-A. Courtemanche, M.-A. Legare, L. Maron, F.-G. Fontaine, *J. Am. Chem. Soc.* 2014, **136**, 10708. (b) R. Shintani, K. Nozaki, *Organometallics* 2013, **32**, 2459. (c) H.-W Suh, L. M. Guard, N. Hazari *Chem. Sci.* 2014, **5**, 3859.

<sup>13</sup> (a) S. Chakraborty, J. Zhang, J. Krause, H. Guan, *J. Am. Chem. Soc.* 2010, **132**, 8872. (b) M. J. Sgro, D. W. Stephan *Angew. Chem. Int. Ed.* 2012, **51**, 11343. (c) C. Das Neves Gomes, E. Biondiaux, P. Thuery, T. Cantat, *Chem. Eur. J.* 2014, **20**, 7098. (d) M. D. Anker, M. Arrowsmith, P. Bellham, M. S. Hill, G. KociokKohn, D. J. Liptrot, M. F. Mahon, C. Weetman *Chem. Sci.* 2014, **5**, 2826–2830. (e) J. A. B. Abdalla, I. M. Riddlestone, R. Tirfoin, S. Aldridge *Angew. Chem. Int. Ed.* 2015, **54**, 5098–5102.

<sup>14</sup> U. Wietelmann, M. Felderhoff, P. Rittmeyer, *Hydrides*. In *Ullmann's Encyclopedia of Industrial Chemistry*; Wiley-VCH, 2016.

<sup>15</sup> A. Klemm, G. Hartmann, L. Lange, *Sodium and Sodium Alloys*. In *Ullmann's Encyclopedia of Industrial Chemistry*; Wiley-VCH, 2000.

<sup>16</sup> Virtually all B–H reagents are ultimately derived from alkali metal hydrides or NaBH<sub>4</sub>. See reference 14.

<sup>17</sup> (a) H. Asakawa, K.-H. Lee, K. Furukawa, Z. Lin, M. Yamashita, *Chem. Eur. J.* 2015, **21**, 4267. (b) C.-W. Chiu, F. P. Gabbai, *Organometallics* 2008, **27**, 1657. (c) C.-W. Chiu, Y. Kim, F. P. Gabbai, *J. Am. Chem. Soc.* 2009, **131**, 60. (d) J. Edwin, M. Bochmann, M. C. Boehm, D. E. Brennan, W. E. Geiger, C. Krueger, J. Pebler, H. Pritzkow, W. Siebert, *J. Am. Chem. Soc.* 1983, **105**, 2582. (e) G. E. Herberich, B. Buller, B. Hessner, W. Oschmann, *J. Organomet. Chem.* 1980, **195**, 253. (f) E. Januszewski, M. Bolte, H.-W. Lerner, M. Holthausen, M. Wagner, *Dalton Trans.* 2013, 42 (38), 13826. (g) R. J. Kwaan, J. C. Harlan, J. R. Norton, *Organometallics* 2001, **20**, 3818. (h) A. Lorbach, A. Hubner, M. Wagner, *Dalton Trans.* 2012, **41**, 6048. (i) P. Muller, B. Gangnus, H. Pritzkow, H. Schulz, M. Stephan, W. Siebert, *J. Organomet. Chem.* 1995, **487**, 235.

<sup>18</sup> Y. Segawa, M. Yamashita, K. Nozaki, *Science* 2006, **314**, 113.

<sup>19</sup> R. Kinjo, B. Donnadieu, M. A. Celik, G. Frenking, G. Bertrand, *Science* 2011, **333**, 610.

<sup>20</sup> L. Kong, Y. Li, R. Ganguly, D. Vidovic, R. Kinjo, *Angew. Chem. Int. Ed.*, 2014, **53**, 9280.

<sup>21</sup> (a) A. Hübner, T. Kaese, M. Diefenbach, B. Endeward, M. Bolte, H.-W. Lerner, M. C. Holthausen, M. Wagner, *J. Am. Chem. Soc.* 2015, **137**, 3705. (b) T. Kaese, H. Budy, M. Bolte, H.-W. Lerner, M. Wagner, *Angew. Chem. Int. Ed.* 2017, **56**, 7546.

<sup>22</sup> (a) T. J. Carter, J. W. Kampf, N. K. Szymczak, *Angew. Chem. Int. Ed.* 2012, **51**, 13168. (b) T. J. Carter, J. Y. Wang, N. K. Szymczak, *Organometallics* 2014, **33**, 1540. (c) T. J. Carter, Z. M. Heiden, N. K. Szymczak, *Chem. Sci.* 2015, **6**, 7258.

<sup>23</sup> J. W. Taylor, A. McSkimming, M.-E. Moret, W. H. Harman, *Angew. Chem. Int. Ed.* 2017, **56**, 10413.

<sup>24</sup> Wagner has recently shown that C-halogenation can render DBA derivatives significantly easier to reduce: S. Brend'amour, J. Gilmer, M. Bolte, H.-W. Lerner, M. Wagner, *Chem. Eur. J.*, 2018, **24**, 16910–16918.

<sup>25</sup> E. von Grotthuss, S. E. Prey, M. Bolte, H.-W. Lerner, M. Wagner, *J. Am. Chem. Soc.* 2019, **141**, 6082.

<sup>26</sup> E. von Grotthuss, S. E. Prey, M. Bolte, H.-W. Lerner, M. Wagner, *Angew. Chem. Int. Ed.* 2018, **57**, 16491.

<sup>27</sup> (a) E. Benson, C. Kubiak, A. Sathrum, J. Smieja, *Chem. Soc. Rev.* 2009, **38**, 89. (b) A. M. Appel, J. E. Bercaw, A. B. Bocarsly, H. Dobbek, D. L. DuBois, M. Dupuis, J. G. Ferry, E. Fujita, R. Hille, P. J. A. Kenis, C. A. Kerfeld, R. H. Morris, C. H. F. Peden, A. R. Portis, S. W. Ragsdale, T. B. Rauchfuss, J. N. H. Reek, L. C. Seefeldt, R. K. Thauer, G. L. Waldrop, *Chem. Rev.* 2013, **113**, 6621. (c) J. Qiao, Y. Liu, F. Hong, J. A. Zhang *Chem. Soc. Rev.* 2014, **43**, 631. (d) C. Costentin, M. Robert, J.-M. Savéant, *Chem. Soc. Rev.* 2013, **42**, 2423.

<sup>28</sup> (a) N. Sreekanth, M. A. Nazrulla, T. V. Vineesh, K. Sailaja, K. L. Phani, *Chem. Commun.* 2015, **51**, 16061. (b) T. B. Tai, M. T. Nguyen, *Chemistry* 2013, **19**, 2942.

<sup>29</sup> (a) J. W. Taylor, A. McSkimming, C. F. Guzman, W. H. Harman, *J. Am. Chem. Soc.* 2017, **139**, 11032. (b) D. Wu, L. Kong, Y. Li, R. Ganguly, R. Kinjo, *Nat. Commun.* 2015, **6**, 7340.

<sup>30</sup> (a) Y. Su, R. Kinjo, *Coord. Chem. Rev.* 2017, **352**, 346. (b) P.-Y. Feng, Y.-H. Liu, T.-S. Lin, S.-M. Peng, C.-W. Chiu, *Angew. Chem. Int. Ed.* 2014, **53**, 6237. (c) Y. Su, Y. Li, R. Ganguly, R. Kinjo, *Chem. Sci.* 2017, **8**, 7419. (d) B. Wang, Y. Li, R. Ganguly, R. D. Webster, R. Kinjo, *Angew. Chem. Int. Ed.* 2018, **57**, 7826.

<sup>31</sup> F. J. Fernández-Alvarez, A. M. Aitani, L. A. Oro, *Catal. Sci. Technol.*, 2014, **4**, 611–624.

<sup>32</sup> A. Schnurr, H. Vitze, M. Bolte, H.-W. Lerner, M. Wagner, *Organometallics* 2010, **29**, 6012.

<sup>33</sup> (a) C. A. Jaska, D. J. H. Emslie, M. J. D. Bosdet, W. E. Piers, T. S. Sorenson, M. Parvez, *J. Am. Chem. Soc.* 2006, **128**, 10885. (b) Z. Zhang, E. S. Penev, B. I. Yakobson, *Chem. Soc. Rev.* 2017, **46**, 6746. (c) V. M. Hertz, M. Bolte, H.-W. Lerner, M. Wagner, *Angew. Chem. Int. Ed.* 2015, **54**, 8800. (d) B. Su, R. Kinjo, *Synthesis* 2017, **49**, 2985.

<sup>34</sup> E. von Grotthuss, M. Diefenbach, M. Bolte, H.-W. Lerner, M. C. Holthausen, M. Wagner, *Angew. Chem. Int. Ed.*, 2016, **55**, 14067–14071.

<sup>35</sup> (a) W. Sattler, G. Parkin, *J. Am. Chem. Soc.* 2011, **133**, 9708. (b) A. N. Kornev, T. A. Chesnokova, E. V. Zhezlova, L. N. Zakharov, G. K. Fukin, Y. A. Kursky, G. A. Domrachev, P. D. Lickiss, *J. Organomet. Chem.* 1999, **587**, 113.